Abdom Imaging 28:580–587 (2003)
DOI: 10.1007/s00261-002-0069-4

Abdominal Imaging

Invited update

CT virtual intravascular endoscopy of abdominal aortic aneurysms treated with suprarenal endovascular stent grafting

Z. Sun,[1] **R. J. Winder,**[2] **B. E. Kelly,**[3] **P. K. Ellis,**[3] **D. G. Hirst**[1]

[1]School of Biomedical Sciences, University of Ulster, Shore Road, Newtownabbey, BT 37 0QB, Northern Ireland, United Kingdom

[2]School of Applied Medical Sciences and Sport Studies, University of Ulster, Shore Road, Newtownabbey, BT 37 0QB, Northern Ireland, United Kingdom

[3]Department of Radiology, Royal Victoria Hospital, Grosvenor Road, Belfast, BT 12 6BA Northern Ireland, United Kingdom

Abstract

Background: We investigated the clinical applications of virtual intravascular endoscopy (VIE) in patients with abdominal aortic aneurysms (AAA) treated by endovascular stent grafting with a suprarenal component.

Methods: Thirty-four patients with AAA undergoing endovascular stent grafting were included in the study (28 male, six female; mean age = 76 years). Helical computed tomography (CT) scanning was performed within 1 week after stent graft implantation. All patients received a Zenith/AAA endovascular graft with uncovered suprarenal struts 2.5 cm long placed around the level of the renal arteries. VIE images were created for each patient. The follow-up periods ranged from 3 to 18 months (mean = 8.3 ± 3.7 months).

Results: Three of 34 celiac arteries, 22 of 34 superior mesenteric arteries, 32 of 34 right renal arteries, and 30 of 35 left renal arteries were affected by the suprarenal stent struts (wires) to different extents. VIE was able to demonstrate the struts, arterial ostia, and the strut/ostia configuration. Follow-up CT showed that all of these aortic branches were patent.

Conclusion: Our preliminary experience has demonstrated that VIE is a novel imaging technique to visualize the three-dimensional intralumenal relationship of the aortic stent struts to the arterial ostia in patients with AAA after suprarenal stent graft placement.

Key words: Aneurysm—Stent—Computed tomography—Virtual endoscopy.

Correspondence to: Z. Sun

In recent years, abdominal aortic aneurysm (AAA) repair has been accomplished by using transfemoral insertion of a stent graft [1–5]. The endovascular exclusion of infrarenal AAA has gained wide acceptance among physicians and patients alike. The potential advantages of endovascular AAA repair have been reported at length and include decreased morbidity, mortality, length of hospital stay, and lower overall treatment cost [6]. However, despite the technical advances achieved in the past decade, the application of endovascular AAA repair remains limited. This is at least partly due to the high proportion of aneurysms with unsuitable aneurysm neck anatomy. A suboptimal neck makes stent graft fixation difficult and jeopardizes the durability of a successful repair. Placement of an uncovered suprarenal component over the renal artery ostia has been demonstrated to improve the fixation of stent graft and reduce the incidence of proximal endoleaks in patients with short and difficult aneurysm necks [7].

Mismatch of the size of the stent graft and the aorta may result in a lack of aneurysm exclusion; therefore, accurate measurements are crucial [8]. Helical computed tomographic angiography (CTA) is generally accepted as the preferred imaging technique for preoperative assessment and the follow-up of patients undergoing treatment with stent graft implants [9, 10]. CT volumetric acquisition has been complemented by the parallel development of image processing and visualization methods to create high-quality images including three-dimensional (3D) representations of anatomic structure [11]. These are multiplanar reformatting, maximum intensity projection (MIP), and virtual endoscopy (VE). The former two reconstruction methods are commonly used to make preoperative measurements [9, 12]. VE is a recently developed 3D technique that can present internal views of image volumes by using a combination of surface shading and

3D perspective. Results of previous investigations have suggested that VE could play a role in the preoperative planning of surgery for AAAs and postoperative follow-up [13, 14]. However, to our knowledge, an investigation of virtual intravascular endoscopy (VIE) in evaluating the relation of the suprarenal stent strut to the arterial ostia has not been performed. We report our preliminary experience of the application of VIE in patients with AAA after suprarenal stent graft placement.

Materials and methods

Patients and scanning protocol

Thirty-four patients (28 men, six women; age range = 63–84 years; mean age = 76 years) who underwent endovascular repair of AAAs were included in the study. Patient assessment was performed by an interventional radiologist and a vascular surgeon with the use of CTA. CTA was performed on a Philips AV-E1 CT scanner in a single breath-hold technique with a beam collimation of 5 mm, a pitch of 1.0, and a reconstruction interval of 2 mm. Contrast enhancement was given to all patients to a total volume of 100 mL, a flow rate of 2 mL/s, and a scan delay of 30 s.

Stent graft and implantation

Suitable patients were treated with a Zenith/AAA endovascular stent graft (Cook Europe, Denmark) with uncovered suprarenal struts. The suprarenal struts consist of metal barbed wires with a length of 2.5 cm placed across the renal arteries, with the intention of taking advantage of the better fixation available at the relatively good quality aorta found around these ostia. All procedures were performed in the operating theater by a collaborative team of vascular surgeons and interventional radiologists. The position of the stent and renal artery patency were confirmed by intraoperative fluoroscopy and angiography.

Virtual intravascular endoscopy

Generation of VIE images of the aortic lumen

VIE images were generated with commercial software (Analyze AVW 3.1, analyzedirect.com) running on a unix workstation (Sun Microsystems, Mountain view, CA, USA). The CT data were prepared for VIE by removing the contrast-enhanced blood from the aorta with a CT number thresholding technique. A CT number threshold range was identified using three regions of interest (ROI) measurements, as shown in Figure 1. Figure 1 A–C shows the locations chosen to be representative of the CT number range of contrast-enhanced blood, i.e., the renal artery, aneurysm body, and aortic bifurcation. Figure 1D shows a graph of the average CT number at the three ROI locations as indicated in Figure 1 A–C. For each patient these three measurements were averaged to produce the threshold value applied to remove the contrast-enhanced blood. Figure 1E shows a surface-shaded caudal view of a CT dataset with the CT number threshold applied. Note that the contrast-enhanced blood has been removed from the major vessels. Also, because of the threshold value chosen, bone information also has been removed, although this does not affect the production of intralumenal views. Because of the threshold chosen to show the lumen surface, the metal stent struts are also removed.

Generation of VIE images of the aortic ostia and stent combined

The CT number of the stent strut in Zenith aortic stents is much higher than that of contrast-enhanced blood. Therefore, different threshold ranges are required to generate VIE images of an aortic stent and lumenal structure. First, a low threshold range, e.g., −1200 to 150 HU, was applied, which removed the contrast-enhanced blood from the aorta. Second, a higher threshold range, e.g., 500 to 2000 HU, was applied to visualize the wire struts only, excluding enhanced blood and lumenal structures. The two individual virtual endoscopic images of lumen and wire were added numerically together, producing a combination of the aortic stent and the aortic lumen (Fig. 2). The registration of lumen and strut images was achieved by using exactly the same viewing coordinates. Figure 2A shows that the left renal ostium was generated with the lower threshold of −1200 HU and the upper threshold of 120 HU to include all the soft tissue and lumen structures and exclude high-density structures such as contrast-enhanced blood and the stent strut. Figure 2B shows the virtual endoscopic image of a stent strut generated by applying a lower threshold of 500 HU and an upper threshold of 2890 HU to include only the high-density metallic struts. Figure 2C shows the VIE combination image in which it is possible to determine the 3D relation of the strut to the ostium. Figure 2C demonstrates direct encroachment of the renal ostium by a stent strut.

Characterization of stent strut/ostia configuration

We characterized the configuration of the stent strut and the ostia into three types. Figure 3A shows diagrammatically two regions within the artery named central (C) and peripheral (P). These characterizations were used because blood flow in the center of an artery is greatest and slowest at the periphery of the vessel lumen (Fig. 3B). If

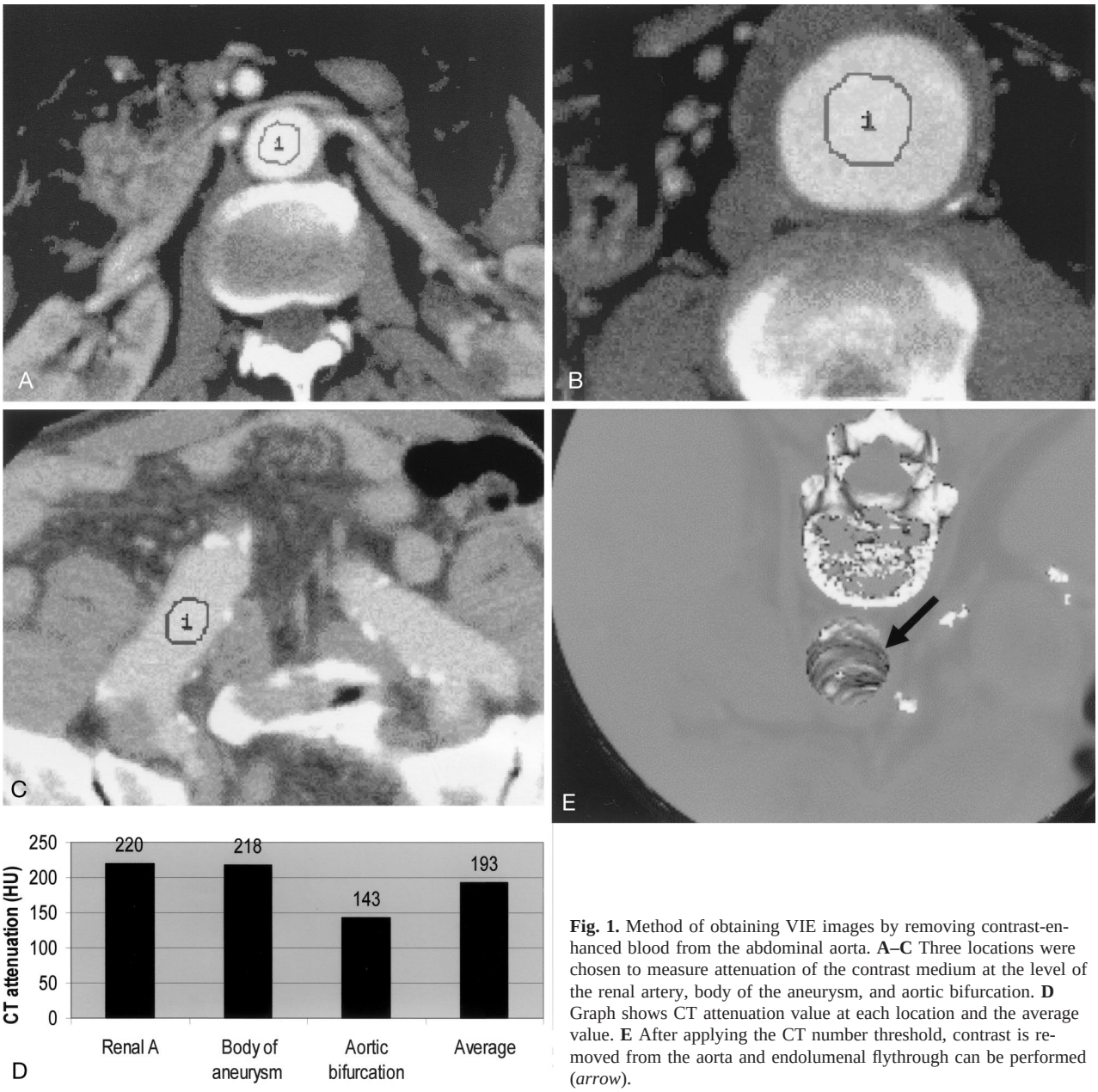

Fig. 1. Method of obtaining VIE images by removing contrast-enhanced blood from the abdominal aorta. **A–C** Three locations were chosen to measure attenuation of the contrast medium at the level of the renal artery, body of the aneurysm, and aortic bifurcation. **D** Graph shows CT attenuation value at each location and the average value. **E** After applying the CT number threshold, contrast is removed from the aorta and endolumenal flythrough can be performed (*arrow*).

the strut crossed the central one-third of the ostium, the configuration was designated C; if the strut crossed the outer two-thirds of the ostium, it was designated P. If the strut did not appear to encroach on the ostium, it was designated no impact (N).

Results

VIE findings of the 3D relation of the stent wire to the ostia

VIE images were successfully generated in all patients and showed the relative positions of the stent wire and renal ostia. The time for creation and analysis of VIE images ranged from 20 to 30 min including threshold measurements and production of combination images. A total of 34 celiac arteries, 34 superior mesenteric arteries (SMA), 34 right renal arteries, and 35 left renal arteries were evaluated on VIE. An accessory renal artery was found to arise from the left side of the aorta in two cases and from the right side in one case. One patient had a previous right nephrectomy and another had a hypoplastic left kidney with no observable renal artery.

The configuration of the strut and ostia was easily identified in 30 patients (Figs. 4–6), whereas image quality was suboptimal in the remaining four cases). This was

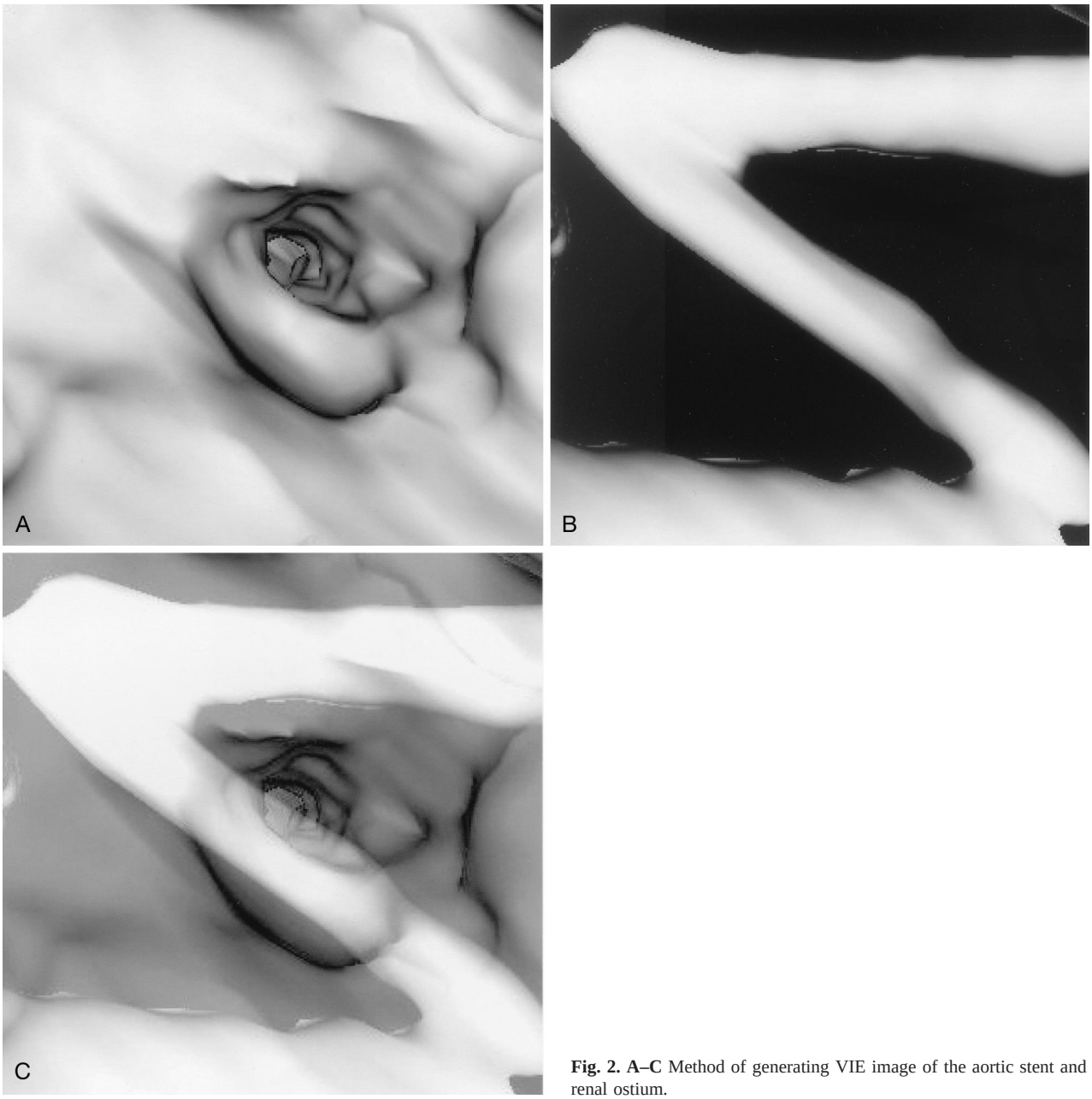

Fig. 2. A–C Method of generating VIE image of the aortic stent and renal ostium.

due to inappropriate contrast enhancement in two (mean CT attenuation of the abdominal aorta $<$ 100 HU) and angulation of the aneurysm neck in another two cases.

Visualization of the stent strut and its spatial relation to the ostia

Table 1 shows the number of the arterial ostia affected by stent struts and the configuration of stent strut/ostia observed with VIE. Nearly all of the celiac ostia were not affected by the placement of the stent graft due to its distal location above the other three branches. In contrast, more than half of the SMA ostia were encroached by struts to various degrees. For renal ostia, only seven of 69 were unaffected. Table 1 also shows the number of struts crossing the aortic branch ostia. More than half of the ostia (49 of 87) were crossed by multiple struts. It was difficult to evaluate exactly the extent of coverage of the ostia by the struts because the wire diameter was overestimated on CT. The actual wire diameter was 0.4 mm, which when measured on CT ranged from 1 to 2 mm. The

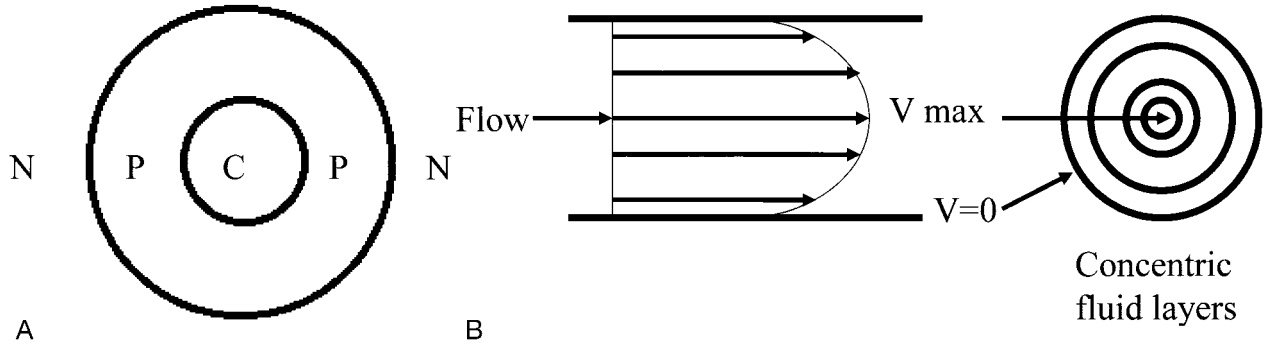

Fig. 3. A Shows the three regions used to characterize the position of the stent wire across the ostium. **B** shows laminar blood flow inside an arterial vessel.

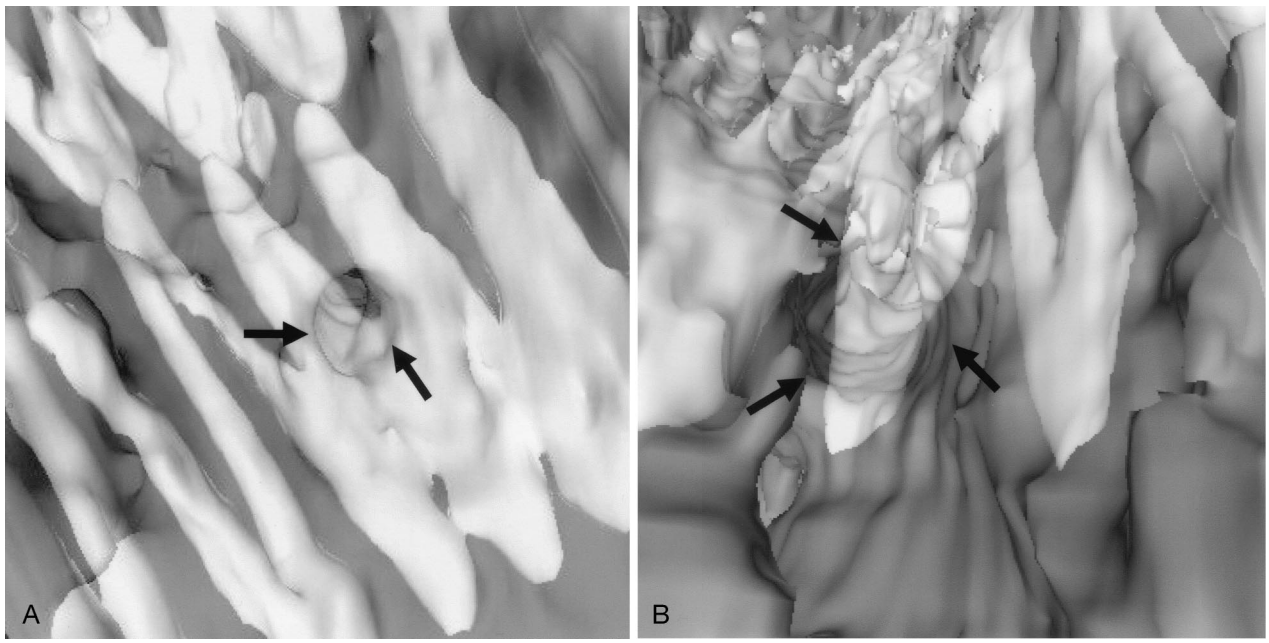

Fig. 4. A shows the left renal ostium crossed centrally by one stent strut, and **B** shows the SMA crossed centrally by multiple struts. *Arrows* indicate the arterial ostium in each image.

overestimation of the struts was caused by the point spread function inherent in CT scanning of small, high-contrast objects.

Follow-up CTA demonstrated that all of the stent-affected aortic branches were patent with no apparent stenosis or occlusion. Follow-up ranged from 3 to 18 months, with a mean period of 8.3 ± 3.7 months.

Discussion

Investigative studies of VIE in pre- and postoperative evaluations of AAAs have been performed [13–17]. It has been suggested that VIE may play a role as a diagnostic tool in endovascular practice. Although VIE has been used to visualize aortic stents in situ, the relation of stent struts to aortic ostia has not previously been demonstrated and required investigation. We believe this could be a potential, valuable application of VIE in aortic stent grafting.

Two of the potential complications of suprarenal stent grafting are the reduction of the cross-sectional area of the vessel ostia by a stent strut and the deposition of endothelial cells with matrix or neointimal hyperplasia around the stent [18]. The SMA, celiac axis, and renal arteries are physically close and normally spaced within 2 cm of each other. It has been reported that nearly 50% of the patients who undergo endovascular repair with a suprarenal com-

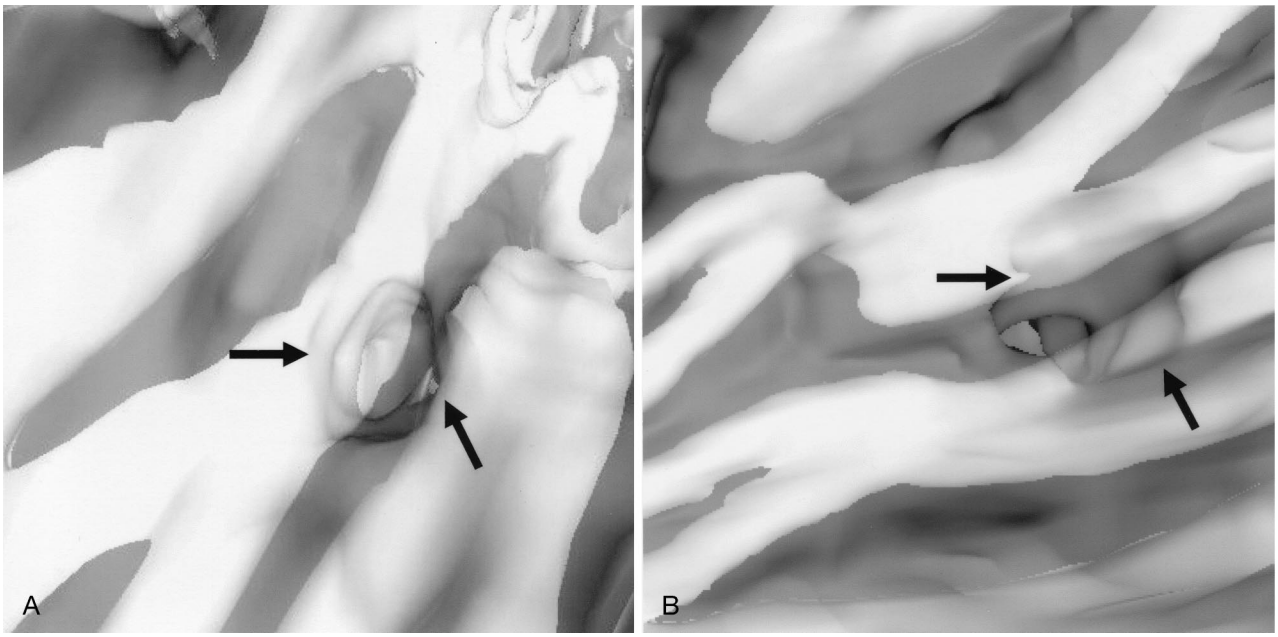

Fig. 5. The right renal ostium affected peripherally by (**A**) one stent strut and (**B**) multiple struts. *Arrows* indicate the right renal ostia.

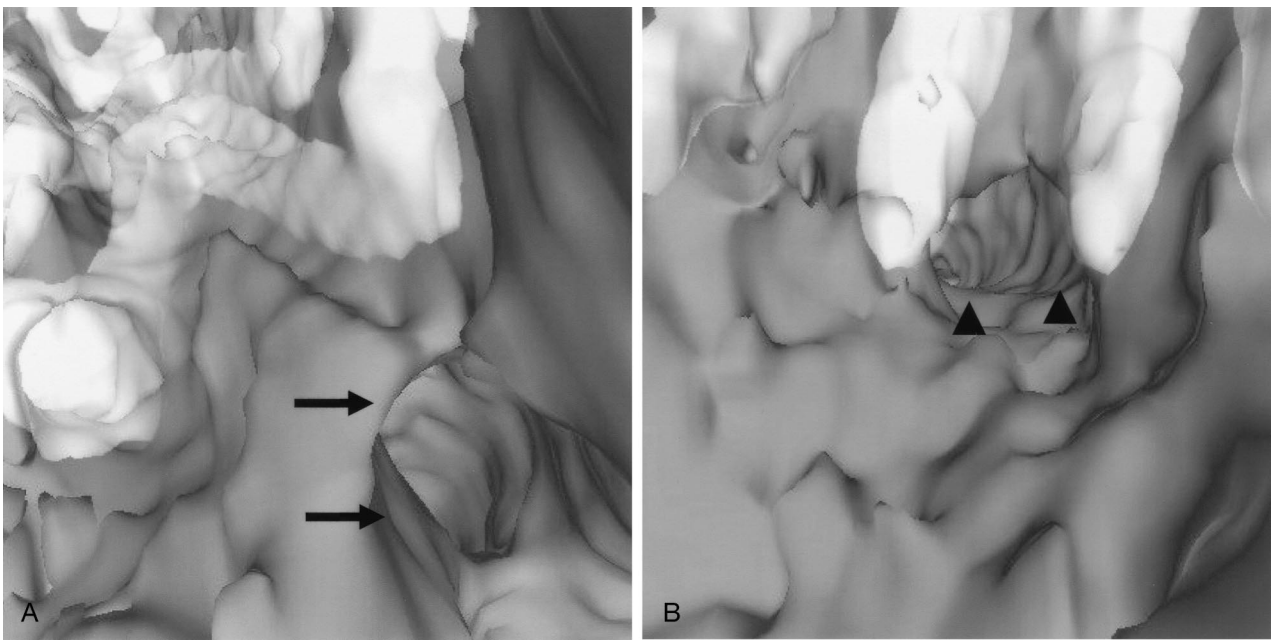

Fig. 6. A and B show no apparent effect on the SMA and the celiac axis, respectively. The celiac axis appears to be partly crossed on this image due to the overestimation of stent thickness. *Arrows* indicate the SMA and *arrowheads* point to the celiac axis.

ponent had most of these visceral branches affected [19]. Our VIE findings in 34 cases supported this observation. Of 137 arterial ostia evaluated in our study, 87 (64%) ostia were affected by struts, and 62 of 87 (71%) were renal ostia. From our observations we noted a range of configurations with which the stent strut may affect the ostia, indicating the random nature of the stent placement.

Figure 3B shows the laminar nature of blood flow within an artery where the greatest velocities are observed at the center of the vessel, with lower velocities at the periphery. We postulate that struts affecting the center of an ostium will have the greatest effect on blood flow. Table 1 shows that more than half of the renal ostia (32 of 62) were affected, as shown in configuration (C), and by

Table 1. Characterization of stent strut/ostia configuration and the number of stent wires crossing the ostia

Arterial ostia	Characterization of strut/ostia configuration			*n* stent wires crossing the ostia	
	C	P	N	Single	Multiple
Celiac	1	2	31	2	1
SMA	15	7	12	4	18
Left renal artery	16	14	5	16	14
Right renal artery	16	16	2	16	16

C, central; N, none; P, peripheral; SMA, superior mesenteric artery

multiple stent struts (30 of 62) based on VIE findings. Further studies are required to determine whether there is any significant difference in blood flow due to the observed configurations of stent strut and ostia.

It has been suggested that a long-term effect may be the deposition of neointimal hyperplasia around stent struts that may affect renal blood flow. However, clinical and experimental studies have suggested that the impact on the renal ostia or renal blood flow depend mainly on the type of stent graft used [20–27]. Using a porcine model, Malina et al. [21] showed that, where aortic stents crossed the renal ostia, there was no effect on renal blood flow in the acute setting. Similar results were reported by Ferko et al. [22] in experimental and clinical experiences. Chronic transrenal stent implantation for up to 36 months in dogs has supported these observations [22, 28]. However, other investigators found that some types of aortic stents might compromise renal perfusion secondary to neointimal formation [20, 26]. It has been reported that the neointima develop around struts crossing the renal ostia from Strecker, Memotherm, and Palmaz stents, with a mean area coverage as high as 43 $\pm$ 30%. Therefore, data derived from examining one stent type may not apply to another model. The Zenith/AAA stent graft used in our study has not been reported to affect renal perfusion or function, although the long-term effect on the renal blood flow is not well established. The benefits and complications of suprarenal stent need to be explored systematically and VIE may be a valuable technique in this area. We are currently assessing medium- to long-term renal function in this group of patients to compare those arteries with strut encroachment with those that are clear.

Our study has revealed intralumenal information concerning the relation of aortic struts to arterial ostia that cannot be obtained by any other imaging method. Conventional angioscopic examination in patients is not practical and routine CT examination does not reveal this detail of information. Its value as a research tool may yet be realized. With the advent of fenestrated stent grafting (where suprarenal aortic aneurysms can be treated by leaving a gap in the graft material to allow passage of stents from the graft into the visceral and renal arteries), the ability of VIE to assess the exact relation of the ostia and cross-sectional appearances may allow a role in planning.

Conclusion

We have presented our preliminary experience of VIE in patients with AAA undergoing suprarenal stent graft placement. VIE was found to be a novel technique in demonstrating the 3D relation of suprarenal stents to the arterial ostia within the aorta. Intralumenal information provided by VIE may aid practitioners in accurately assessing the degree of encroachment of suprarenal struts on the renal and other visceral ostia. This would allow accurate correlation with clinical and biochemical findings. In addition, with fenestrated stent–grafting emerging, a role for VIE in graft planning may evolve.

References

1. Moore WS, Vescera CL. Repair of abdominal aortic aneurysm by transfemoral endovascular graft placement. *Ann Surg* 1994;220: 331–341
2. Moore WS, Rutherford RB, for the EVT Investigators. Transfemoral endovascular repair of abdominal aortic aneurysms: results of the North American EVT phase 1 trial. *J Vasc Surg* 1996;23:543–553
3. Chuter TA, Wendt G, Hopkinson BR, et al. Bifurcated stent-graft for abdominal aortic aneurysm. *Cardiovasc Surg* 1997;5:388–392
4. Blum U, Voshage G, Lammer J, et al. Two-centre German experience with aortic endografting. *J Endovasc Surg* 1997;4:137–146
5. Marin ML, Veith FJ, Cynamon J, et al. Initial experience with transluminally placed endovascular grafts for the treatment of complex vascular lesions. *Ann Surg* 1995;222:449–469
6. Parodi JC, Palmaz JC, Barone HD. Transfemoral intraluminal graft implantation for abdominal aortic aneurysms. *Ann Vasc Surg* 1991; 5:491–499
7. Marin ML, Parsons RE, Hollier LH, et al. Impact of transrenal aortic endograft placement on endovascular graft repair of abdominal aortic aneurysms. *J Vasc Surg* 1998;28:638–646
8. Seelig MH, Oldenburg WA, Hakaim AG, et al. Endovascular repair of abdominal aortic aneurysms: where do we stand? *Mayo Clin Proc* 1999;74:999–1010
9. Broeders IAMJ, Blankensteijn JD, Olree M, et al. Preoperative sizing of grafts for transfemoral endovascular aneurysm management: a prospective comparative study of spiral CT angiography, arterial angiography and conventional CT imaging. *J Endovasc Surg* 1997;4:252–261
10. Armerding MD, Rubin GD, Beaulieu CF, et al. Aortic aneurysmal disease: assessment of stent-grafted treatment-CT versus conventional angiography. *Radiology* 2000;215:138–146
11. Bartolozzi C, Neri E, Caramella D. CT in vascular pathologies. *Eur Radiol* 1998;8:679–684
12. Beebe HG, Kritpracha B, Serres S, et al. Endograft planning without preoperative arteriography: a comparative feasibility study. *J Endovasc Ther* 2000;7:8–15
13. Neri E, Bonanomi C, Vignali R, et al. Spiral CT virtual endoscopy of abdominal arteries: clinical applications. *Abdom Imaging* 2000; 25:59–61
14. Beier J, Diebold T, Vehse H, et al. Virtual endoscopy in the assessment of implanted aortic stents. CAR '97, Computer Assisted

Radiology and Surgery, Proceedings of the 11th International Symposium and Exhibition, Lenke HU et al (eds) 1997;183–185
15. Davis CP, Ladd ME, Romanowski BJ, et al. Human aorta: preliminary results with virtual endoscopy based on three-dimensional MR imaging data sets. *Radiology* 1996;199:37–40
16. Rubin GD, Beaulieu CF, Argiro V, et al. Perspective volume rendering of CT and MR images: applications for endoscopic imaging. *Radiology* 1996;199:321–330
17. Neri E, Caramella D, Bisogni C, et al. Detection of accessory renal arteries with virtual vascular endoscopy of the aorta. *Cardiovasc Intervent Radiol* 1999;22:1–6
18. Kalliafas S, Travis SJ, Macierewicz J, et al. Intrarenal color duplex examination of aortic endograft patients with suprarenal stents. *J Endovasc Surg* 2001;8:592–596
19. Kramer SC, Seifarth H, Pamler R, et al. Renal infarction following endovascular aortic aneurysm repair: incidence and clinical consequences. *J Endovasc Ther* 2002;9:98–102
20. Birch PC, Start RD, Whitebread T, et al. The effect of crossing porcine renal artery ostia with various endovascular stents. *Eur J Vasc Endovasc Surg* 1999;17:185–190
21. Malina M, Lindh M, Ivancev K, et al. The effects of endovascular aortic stents placed across the renal arteries. *Eur J Vasc Endovasc Surg* 1997;13:207–213
22. Ferko A, Krajina A, Jon B, et al. Juxtarenal aortic aneurysm: endoluminal transfemoral repair? *Eur Radiol* 1997;7:703–707
23. Duda SH, Raygrotzki S, Wiskirchen J, et al. Abdominal aortic aneurysms: treatment with juxtarenal placement of covered stent grafts. *Radiology* 1998;206:195–198
24. Lobato AC, Quick RC, Vaughn PL, et al. Transrenal fixation of aortic endografts: intermediate follow-up of a single-center experience. *J Endovasc Ther* 2000;7:273–278
25. Whitbread T, Birch P, Rogers S, et al. The effect of placing an aortic wall stent across the renal artery origins in an animal model. *Eur J Vasc Endovasc Surg* 1997;13:154–158
26. Desgranges P, Hutin E, Kedzia C, et al. Aortic stents covering the renal arteries ostia: an animal study. *J Vasc Intervent Radiol* 1997; 8:77–82
27. Bove PG, Long GW, Zelenock GB, et al. Transrenal fixation of aortic stent-grafts for the treatment of infrarenal aortic aneurysmal disease. *J Vasc Surg* 2000;7:697–203
28. Mirich D, Wright KC, Wallace S, et al. Percutaneously placed endovascular grafts for aortic aneurysms: feasibility study. *Radiology* 1989;170:1033–1037